901274

NAWCWPNS TP 8098

An Introduction to Wideband Ambiguity Functions and Time-Scale Representations for Radar/Sonar Applications

by
Brett Borden
Physics Division
Research Department

JANUARY 1993

NAVAL AIR WARFARE CENTER WEAPONS DIVISION
CHINA LAKE, CA 93555-6001

Naval Air Warfare Center Weapons Division

FOREWORD

The research described in this report was performed during fiscal year 1993 as part of an effort to improve upon radar classification and identification of noncooperative targets. This problem continues to be a primary goal of radar research programs, and considerable effort has been expended within the last few decades in attempts to solve it. Invariably, the accuracy of these methods depends upon available radar resolution and so, indirectly, it depends on radar bandwidth.

Many classical results in radar systems theory presume that the narrowband approximation is valid. It is hoped that this report will help clarify what is gained and what is lost when this approximation is not valid. The results, while not surprising, also offer an interesting interpretation in terms of "wavelet" (or time-scale) representations. This effort was supported by the Office of Naval Research.

This report has been reviewed for technical accuracy by Gary A. Hewer.

Approved by
R. L. DERR, *Head*
Research Department
15 January 1993

Under authority of
W. E. NEWMAN
RAdm., U.S. Navy
Commander

Released for publication by
S. HAALAND
Deputy Commander for Research & Development

NAWCWPNS Technical Publication 8098

Published by ..... Technical Information Department
Collation ..... Cover, 17 leaves
First printing ..... 65 copies

REPORT DOCUMENTATION PAGE

Form Approved
OMB No. 0704-0188

1. AGENCY USE ONLY *(Leave blank)*	2. REPORT DATE	3. REPORT TYPE AND DATES COVERED
	January 1993	Interim Oct—Dec 1992

4. TITLE AND SUBTITLE
AN INTRODUCTION TO WIDEBAND AMBIGUITY FUNCTIONS AND TIME-SCALE REPRESENTATIONS FOR RADAR/SONAR APPLICATIONS

5. FUNDING NUMBERS
WU 113132
PE 61153N
TA BR052-02-01

6. AUTHOR(S)
Brett Borden

7. PERFORMING ORGANIZATION NAME(S) AND ADDRESS(ES)
Naval Air Warfare Center Weapons Division
China Lake, CA 93555-6001

8. PERFORMING ORGANIZATION REPORT NUMBER
NAWCWPNS TP 8098

9. SPONSORING/MONITORING AGENCY NAME(S) AND ADDRESS(ES)
Office of Naval Research
Arlington, VA 22217-5000

10. SPONSORING/MONITORING AGENCY REPORT NUMBER

11. SUPPLEMENTARY NOTES

12A. DISTRIBUTION/AVAILABILITY STATEMENT
A Statement; public release; distribution unlimited

12B. DISTRIBUTION CODE

13. ABSTRACT *(Maximum 200 words)*

(U) Recent advancements in the ability of radar/sonar systems to launch and analyze signals of very short time duration have caused many to re-examine the so-called wideband ambiguity function. Much of this work has been at a mathematical level that has placed it out of reach to many radar and sonar engineers. Some of the work has been incomplete—occasionally even incorrect. Our present pedagogical discussion uses the standard time-frequency motivation for time-scale distributions. We compare and contrast the usual narrowband techniques with the wideband approach and explain how high-resolution downrange imaging requires an understanding of the latter.

14. SUBJECT TERMS
Ambiguity function
Wideband
Wavelet

15. NUMBER OF PAGES
32

16. PRICE CODE

17. SECURITY CLASSIFICATION OF REPORT	18. SECURITY CLASSIFICATION OF THIS PAGE	19. SECURITY CLASSIFICATION OF ABSTRACT	20. LIMITATION OF ABSTRACT
UNCLASSIFIED	UNCLASSIFIED	UNCLASSIFIED	UL

CONTENTS

1. INTRODUCTION

Within the last few years there has been a renewal of interest in wideband radar systems and techniques (References 1 through 3). This interest is largely because of the prospects for high-resolution downrange target imaging that, because of technological advancements in signal generation and processing, are only now becoming feasible. It is also due to inherent differences between the natural representations of narrowband and wideband radar signals and a new appreciation of how these differences might be exploited.

The purpose of the present discussion is to examine some of the results from this field that are relevant to the applied problem of increased resolution in radar target imaging. Much of the recent work in wideband ambiguity functions has had a decidedly mathematical flavor that, regrettably, has put it out of the reach of many of the radar engineers who might be expected to benefit most from it. We shall avoid this approach whenever possible and choose explanations that are more "classical" in appearance. This means that we will invariably be less accurate in our definitions, and the reader is advised to refer back to the original references for completeness.

We begin by briefly reviewing the standard time-frequency methods in signal processing. We shall make no attempt to reference all of the important achievements made by the many researchers in this field; instead, we refer the interested reader to the excellent review of this material presented in Reference 4. In Section 5 we introduce the wideband and narrowband ambiguity functions. These functions are keys to understanding radar imaging, and we will show how they are related and how they differ. While the narrowband ambiguity function is understandable in terms of time-frequency methods, we will see that the wideband ambiguity function requires time-scale techniques. In Sections 6 and 7 we will explore some of the differences between time-frequency and time-scale representations and argue for choosing the latter in high-resolution imaging applications.

2. PROBLEM STATEMENT

For a signal $s(t)$, denote by $|s(t)|^2$ the "instantaneous power" at time t and by $|\hat{s}(\omega)|^2$ the "power spectrum" at ω. We seek to determine a function $P(t,\omega)$, called the time-frequency distribution, which satisfies the marginal relations

$$\int_{-\infty}^{\infty} P(t,\omega)d\omega = |s(t)|^2, \qquad \int_{-\infty}^{\infty} P(t,\omega)dt = |\hat{s}(\omega)|^2, \tag{2.1}$$

and such that the total energy of the signal is given by

$$E = \int_{-\infty}^{\infty}\int_{-\infty}^{\infty} P(t,\omega)d\omega\,dt\ . \tag{2.2}$$

For stochastic signals, these results reduce to their probabilistic form. For deterministic signals, this distribution is really an energy density; the "distribution" nomenclature, though partly a holdover from quantum mechanics, is used because the global average (the expectation) of a function $g(t,\omega)$ is defined by

$$\langle g\rangle \equiv \int_{-\infty}^{\infty}\int_{-\infty}^{\infty} g(t,\omega)P(t,\omega)dt\,d\omega\ . \tag{2.3}$$

The local or conditional mean at a particular time is defined by

$$\langle g\rangle_t \equiv \frac{\int_{-\infty}^{\infty} g(t,\omega)P(t,\omega)d\omega}{\int_{-\infty}^{\infty} P(t,\omega)d\omega} \tag{2.4}$$

(and similarly for the mean at a particular frequency).

Equations 2.3 and 2.4 are the main motivations for seeking $P(t,\omega)$.

3. DERIVATION OF $P(t,\omega)$

The characteristic function is the expectation of $e^{i(\theta t+\tau\omega)}$:

$$M(\theta,\tau) \equiv \int_{-\infty}^{\infty}\int_{-\infty}^{\infty} e^{i(\theta t+\tau\omega)}P(t,\omega)dt\,d\omega\ . \tag{3.1}$$

Characteristic functions are convenient because joint moments can be calculated by differentiation:

$$\langle t^n \omega^m \rangle = \frac{1}{i^{n+m}} \frac{\partial^{n+m}}{\partial \theta^n \partial \tau^m} M(\theta, \tau)\Big|_{\theta,\tau=0} \quad , \tag{3.2}$$

and so, expanding the exponential in Equation 3.1 in a Maclaurin series reveals that they may be expressed as

$$M(\theta, \tau) = \sum_{n=0}^{\infty} \sum_{m=0}^{\infty} \frac{(i\theta)^n (i\tau)^m}{n!\, m!} \langle t^n \omega^m \rangle \quad . \tag{3.3}$$

For functions $g_1(t)$ and $g_2(\omega)$, we have

$$\langle g_1(t) \rangle = \int_{-\infty}^{\infty} |s(t)|^2 g_1(t)\, dt = \int_{-\infty}^{\infty} \hat{s}^*(\omega) g_1\left(i \frac{d}{d\omega}\right) \hat{s}(\omega)\, d\omega \tag{3.4}$$

and

$$\langle g_2(\omega) \rangle = \int_{-\infty}^{\infty} |\hat{s}(\omega)|^2 g_2(\omega)\, d\omega = \int_{-\infty}^{\infty} s^*(t) g_2\left(-i \frac{d}{dt}\right) s(t)\, dt \quad . \tag{3.5}$$

Consequently, we can associate time and frequency with the operators T and W, so that

$$\begin{aligned} &T \to t \qquad W \to -i\frac{d}{dt} \qquad \text{in the time domain} \\ &T \to i\frac{d}{d\omega} \qquad W \to \omega \qquad \text{in the frequency domain.} \end{aligned} \tag{3.6}$$

A function $g(t, \omega)$ of both time and frequency may be formally treated in the same way:

$$\langle g(t, \omega) \rangle = \int_{-\infty}^{\infty} s^*(t) G(t, W) s(t)\, dt = \int_{-\infty}^{\infty} \hat{s}^*(\omega) G(T, \omega) \hat{s}(\omega)\, d\omega \quad , \tag{3.7}$$

where $G(T, W)$ is the operator "associated" with $g(t, \omega)$. Equation 3.3 allows us to write

$$M(\theta,\tau)=\left\langle e^{i(\theta t+\tau\omega)}\right\rangle \rightarrow \int_{-\infty}^{\infty} s^{*}(t)e^{i\theta t}\,e^{i\tau W}\,s(t)\,dt$$

or

$$M(\theta,\tau)=\left\langle e^{i(\theta t+\tau\omega)}\right\rangle \rightarrow \int_{-\infty}^{\infty} \hat{s}^{*}(\omega)e^{i\theta T}\,e^{i\tau\omega}\,\hat{s}(\omega)\,d\omega\ . \tag{3.8}$$

However, there is an inherent ambiguity in Equation 3.8 because the association $g(t,\omega)\rightarrow G(T,W)$ is not unique. (For example, Equation 3.3 also allows us to choose $e^{i(\theta t+\tau\omega)}\rightarrow e^{i(\theta T+\tau W)}$.) An unambiguous procedure for the association of $G(T,W)$ with $g(t,\omega)$ sets (References 4 and 5)

$$G(T,W)=\int_{-\infty}^{\infty}\int_{-\infty}^{\infty}\gamma(\theta,\tau)\phi(\theta,\tau)e^{i(\theta T+\tau W)}\,d\theta\,d\tau\ , \tag{3.9}$$

where

$$\gamma(\theta,\tau)\equiv\frac{1}{4\pi^{2}}\int_{-\infty}^{\infty}\int_{-\infty}^{\infty}g(t,\omega)e^{-i(\theta t+\tau\omega)}\,dt\,d\omega \tag{3.10}$$

and $\phi(\theta,\tau)$ is a function, called the kernel, that must satisfy certain initial conditions if the correct marginals are to be obtained (see below).

In the time domain, the operator $e^{i\tau W}$ is the translation operator [i.e., $e^{i\tau W}\,s(t)=e^{\tau(d/dt)}s(t)=s(t+\tau)$] and substitution results in the general form for the characteristic function as

$$M(\theta,\tau)=\phi(\theta,\tau)\int_{-\infty}^{\infty}s^{*}(u)e^{i\theta u}\,s(u+\tau)\,du\ . \tag{3.11}$$

Inverting Equation 3.1 with $M(\theta,\tau)$ given by Equation 3.11 yields the associated general form for distributions:

$$P(t,\omega)=\frac{1}{4\pi^{2}}\int_{-\infty}^{\infty}\int_{-\infty}^{\infty}\int_{-\infty}^{\infty}e^{-i(\theta t+\tau\omega-\theta u)}\,\phi(\theta,\tau)s^{*}(u)s(u+\tau)\,du\,d\tau\,d\theta. \tag{3.12}$$

There are other forms that are used frequently to define this so-called *Cohen's class* of time-frequency distributions. For example, we can write

$$P(t,\omega)=\frac{1}{2\pi}\int_{-\infty}^{\infty}\int_{-\infty}^{\infty}W(u,\omega)\phi(\theta,\tau)e^{-i\theta(t-u)}\,du\,d\theta\ , \tag{3.13}$$

where

$$W(u,\omega)\equiv\frac{1}{2\pi}\int_{-\infty}^{\infty}s^{*}(u)s(u+\tau)e^{-i\tau\omega}\,d\tau \tag{3.14}$$

is the Wigner-Ville distribution. In this form, the factor $\phi(\theta,\tau)e^{-i\theta(t-u)}$ may be interpreted as a "smoothing taper."

Another form writes

$$P(t,\omega)=\frac{1}{2\pi}\int_{-\infty}^{\infty}\int_{-\infty}^{\infty}\chi(\theta,\tau)\phi(\theta,\tau)e^{-i(\theta t+\tau\omega)}\,d\theta\,d\tau\ , \tag{3.15}$$

where

$$\chi(\theta,\tau)\equiv\frac{1}{2\pi}\int_{-\infty}^{\infty}s^{*}(u)s(u+\tau)e^{i\theta u}\,du \tag{3.16}$$

is the (narrowband) ambiguity function, which will be discussed in detail below.

4. KERNEL FUNCTION

The properties of the distribution function are a direct consequence of the choice of kernel. This kernel, in turn, cannot be chosen at will but must obey certain integration and transformation criteria. In particular, the kernel determines whether the density is correctly related to the instantaneous energy and spectrum (References 4 and 5).

Integration of $P(t,\omega)$ with respect to ω yields

$$\int P(t,\omega)\,d\omega = \frac{1}{2\pi}\iiint \delta(\tau)e^{i\theta(u-t)}\,\phi(\theta,\tau)s^*(u)s(u+\tau)\,d\theta\,du\,d\tau$$

$$= \frac{1}{2\pi}\iint e^{i\theta(u-t)}\,\phi(\theta,0)|s(u)|^2\,d\theta\,du. \tag{4.1}$$

If this is to equal $|s(t)|^2$, then

$$\frac{1}{2\pi}\int e^{i\theta(u-t)}\,\phi(\theta,0)\,d\theta = \delta(t-u) \Rightarrow \phi(\theta,0) = 1\,. \tag{4.2}$$

Similarly, it is easy to show that $\phi(0,\tau) = 1$.

We assume throughout that $s(t)$ is normalized to unit energy, and so it also follows that

$$\int P(t,\omega)\,d\omega\,dt = 1 = \text{total energy} \Rightarrow \phi(0,0) = 1\,. \tag{4.3}$$

If we require $P(t,\omega)$ to be real (as is appropriate for a description of energy density), then $\phi(\theta,\tau) = \phi^*(-\theta,-\tau)$.

EXAMPLE 4.1

If we choose $\phi(\theta,\tau) = 1$, then we obtain the Wigner-Ville distribution (References 4, 6, and 7):

$$P_{WV}(t,\omega) = \frac{1}{2\pi}\int_{-\infty}^{\infty} e^{-i\tau\omega}s^*(t)s(t+\tau)\,d\tau\,. \tag{4.4}$$

The Wigner-Ville distribution has been very well studied, and it is known that it may introduce reconstruction artifacts for multicomponent signals (References 4, 8, and 9). In particular, this distribution suffers in that it may not be zero even when the signal is. ♦

EXAMPLE 4.2

The Choi-Williams distribution results from setting $\phi(\theta,\tau)=e^{-\theta^2\tau^2/\sigma}$ so that (References 4 and 9)

$$P_{CW}(t,w)\frac{1}{4\pi^{3/2}}\int_{-\infty}^{\infty}\int_{-\infty}^{\infty}\sqrt{\frac{\sigma}{\tau^2}}\,e^{-\sigma(u-t)^2/4\tau^2-i\omega\tau}s^*(u)s(u+\tau)\,du\,d\tau\,. \tag{4.5}$$

The Choi-Williams distribution can be thought of as a "smoothed" Wigner-Ville distribution with the parameter σ chosen to control spurious cross-terms. ♦

EXAMPLE 4.3

The choice $\phi(\theta,\tau)=e^{i\theta\tau}$ results in the Kirkwood-Rihaczek distribution (References 4, 10, and 11):

$$P_{KR}(t,\omega)=\frac{1}{\sqrt{2\pi}}e^{-i\omega t}\,s(t)\hat{s}^*(\omega)\,. \tag{4.6}$$

This is sometimes called the *complex energy spectrum.* ♦

The distributions of Examples 4.1 through 4.3 result in the correct marginal distributions. Moreover, the Wigner-Ville and Choi-Williams distributions are also real valued. However, these distributions generally are not positive and it may be difficult to interpret expectations based upon them (Reference 4). A distribution that *is* always positive is the spectrogram.

EXAMPLE 4.4

The spectrogram,

$$P_{Spect}(t,\omega)=\left|\frac{1}{\sqrt{2\pi}}\int_{-\infty}^{\infty}e^{-i\omega\tau}s(\tau)h(\tau-t)d\tau\right|^2\,, \tag{4.7}$$

is obtained from

$$\phi(\theta,\tau)=\int_{-\infty}^{\infty}e^{-i\theta u}\,h(u+\tau)h^*(u)du\,. \tag{4.8}$$

The spectrogram is generally an easy-to-interpret distribution. However, its flaw is that it does not yield the correct marginals (satisfying $\phi(\theta,0)=\phi(0,\tau)=1$ requires that $|h(t)|^2=\delta(t)$ *and* $|\hat{h}(\omega)|^2=\delta(\omega)$, and this is impossible). In practice, the "window" $h(t)$ is tailored to a particular application with $|h(t)|^2$ looking "more like" a delta function if good time resolution is desired and $|\hat{h}(\omega)|^2$ looking more like a delta function if good frequency resolution is needed. ♦

A positive distribution that does yield the correct marginals is

$$P(t,\omega)=|s(t)|^2|\hat{s}(\omega)|^2 . \tag{4.9}$$

This distribution is determined *only* by its marginals and so lacks time-frequency correlation information (resulting in possible artifacts in signal reconstruction). In addition, this distribution is not bilinear. In fact, it is impossible to have positive joint distributions with correct marginals, which are bilinear in $s(t)$. However, it *is* possible to satisfy positivity with correct marginals when $\phi(\theta,\tau)$ is a functional of $s(t)$. In this case, Equation 4.9 can be generalized (References 12 and 13), although a systematic procedure for incorporating the correlation information has not been developed (Reference 4).

For any desired expectation, the spectrogram will yield only an average over the extent of the window and can be relied upon only when the signal is short-time stationary (Reference 8). While the spectrogram does not satisfy the marginals, its positivity is a very useful feature. In addition, it is known that the derivative of the phase does not always correspond to the frequency in the Fourier spectrum and so there may be an inherent inconsistency with our original requirement that the distribution satisfy the marginal constraints (References 4 and 14). Consequently, in the following, we shall prefer interpretability over "correctness"—especially since it is recognized that the current theory is not fully consistent and requires considerable further research (Reference 4).

The behavior of the kernel and associated distribution functions under various transformations of the signal are listed in Table 4.1 (c.f., Reference 4).

TABLE 4.1. Properties of Distributions for Transformations of the Signal.

Transformation	$s(t)$	$P(t,\omega)$	$\phi(\theta,\tau)$
Time shift	$s(t+t_o)$	$P(t+t_o,\omega)$	Any
Frequency shift	$\hat{s}(\omega+\omega_o)$ or $s(t)e^{i\omega_o t}$	$P(t,\omega+\omega_o)$	Any
Time scaling	$\sqrt{\lvert\alpha\rvert}s(\alpha t)$	$P(\alpha t,\omega/\alpha)$	$\phi(\theta/\alpha,\alpha\tau)=\phi(\theta,\tau)$
Freq. scaling	$\sqrt{\lvert\beta\rvert}\hat{s}(\beta\omega)$ or $\frac{1}{\sqrt{\lvert\beta\rvert}}s(t/\beta)$	$P(t/\beta,\beta\omega)$	$\phi(\beta\theta,\tau/\beta)=\phi(\theta,\tau)$
Time inversion	$s(-t)$	$P(-t,-\omega)$	$\phi(-\theta,-\tau)=\phi(\theta,\tau)$
Complex conj.	$s^*(t)$	$P(t,-\omega)$	$\phi(\theta,-\tau)=\phi(\theta,\tau)$

Finally, and for completeness, we need to discuss the so-called uncertainty principle. This relationship between the standard deviation of a function and the standard deviation of its Fourier transform is (Reference 4)

$$\left(\int_{-\infty}^{\infty}(t-\bar{t})^2|s(t)|^2\,dt\right)\left(\int_{-\infty}^{\infty}(\omega-\bar{\omega})^2|\hat{s}(\omega)|^2\,d\omega\right)\geq\frac{1}{2} \tag{4.10}$$

for any signal $s(t)$.

The uncertainty principle is a relationship concerning the marginals and expresses the well-known result that a function and its Fourier transform cannot be made arbitrarily narrow.

5. (RADAR) CROSS-AMBIGUITY FUNCTION

For a point target at distance r from a stationary radar and moving with downrange speed v, $|v| << c$, the echo returned from a transmitted pulse $w(t)$ is given by (References 1 through 3, 15 through 17)

$$e(t) = \sqrt{\frac{c-v}{c+v}}\, w\left(\left[\frac{c-v}{c+v}\right]t - \frac{2r}{c+v}\right). \tag{5.1}$$

(The scale factor is required for conservation of energy.) This is an exact result and can be written as

$$e(t) = \sqrt{D}\, w\big(D(t+T)\big)\,, \tag{5.2}$$

where $D = (c-v)/(c+v)$ is the "Doppler stretch factor" and $T = -2r/(c-v)$ is the signal delay at $t = 0$.

The cross-correlation of a test pulse $f_m = \sqrt{a}\, w_m(a(u+t))$ with a point target echo $e_n(t)$ from $w_n(t)$ is

$$\begin{aligned}\langle e_n, f_m\rangle &= \int_{-\infty}^{\infty} \sqrt{D}\, w_n(D(u+T))\sqrt{a}\, w_m^*(a(u+t))\,du \\ &= \sqrt{\frac{D}{a}} \int_{-\infty}^{\infty} w_n\left(\frac{D}{a}(u + a(T-t))\right) w_m^*(u)\,du\,.\end{aligned} \tag{5.3}$$

If we define the *wideband cross-ambiguity function* by (References 1 through 3, 17)

$$A_{nm}(\tau,\alpha) \equiv \sqrt{\alpha} \int_{-\infty}^{\infty} w_n(\alpha(u+\tau))\, w_m^*(u)\,du\,, \tag{5.4}$$

then we can write

$$\langle e_n, f_m\rangle(t,a) = A_{nm}\left(a(T-t), \frac{D}{a}\right). \tag{5.5}$$

The *narrowband* cross-ambiguity function $\chi_{nm}(\tau,\omega)$ can be obtained from Equation 5.4 by writing both w_m and w_n in the form $w(t)=s(t)e^{i\omega_o t}$, where ω_o may be interpreted as a carrier frequency (but need not be). Substitution yields

$$A_{nm}(\tau,\alpha)=\sqrt{\alpha}\,e^{i\omega_o\alpha\tau}\int_{-\infty}^{\infty}s_n(\alpha(u+\tau))s_m^*(u)e^{i\theta u}\,du\,, \tag{5.6}$$

where $\theta\equiv(\alpha-1)\omega_o$. Expanding $s_n(\alpha(u+\tau))$ in powers of $\varepsilon=2v/(c+v)$ and dropping all but the lowest order term (i.e., restricting $s(t)$ to be slowly varying with t in comparison to the exponential factor) results in (Reference 17)

$$\chi_{nm}(t,\theta)\equiv\frac{1}{2\pi}\int_{-\infty}^{\infty}s_n(u+t)s_m^*(u)e^{i\theta u}\,du=\frac{A_{nm}(t/\alpha,\alpha)e^{-i\omega_o t}}{2\pi\sqrt{\alpha}}+o(\varepsilon)\,. \tag{5.7}$$

[Note that the narrowband ambiguity function ($n=m$) is the characteristic function of the Wigner distribution. The "generalized" ambiguity function is the characteristic function of the associated time-frequency distribution (Reference 18).]

If the echo signal is from a collection of moving scatterers with reflectivity density $\rho(T,D)$ defined in such a way that

$$e_n(t)=\int_0^{\infty}\int_{-\infty}^{\infty}\rho(T,D)\sqrt{D}\,w_n(D(t+T))\frac{dT\,dD}{D}\,, \tag{5.8}$$

then it is easy to show that

$$\langle e_n,f_m\rangle(t,a)=\int_0^{\infty}\int_{-\infty}^{\infty}\rho(T,D)A_{nm}\left(a(T-t),\frac{D}{a}\right)\frac{dT\,dD}{D}\,. \tag{5.9}$$

(The measure $dT\,dD/D$ has important consequences later on and is motivated in the Appendix.)

The quantity $\langle e_n, f_m \rangle$ is known as the *reflectivity image* and can be seen to be the actual reflectivity density filtered by the cross-ambiguity function. In practice, this image is obtained by cross-correlating the return signal with a *family* of time-scaled and shifted test pulses and will be examined in more detail below.

The reflectivity image is generally complex-valued. For many purposes, we are more interested in the intensity image:

$$|\langle e_n, f_m \rangle|^2 = \int_0^\infty \int_{-\infty}^\infty \int_0^\infty \int_{-\infty}^\infty \rho(T,D)\rho^*(T',D') \times$$

$$\times A_{nm}\left(a(T-t), \frac{D}{a}\right) A_{nm}^*\left(a(T'-t), \frac{D'}{a}\right) \frac{dT'\,dD'}{D'} \frac{dT\,dD}{D}. \tag{5.10}$$

A common model for the reflectivity density assumes point sources so that

$$\rho(T,D)\rho^*(T',D') = \sigma^2(T,D)\delta(T-T', D-D'), \tag{5.11}$$

where σ^2 is the target cross-section density. Substitution of Equation 5.11 into 5.10 yields the (model-based) result

$$|\langle e_n, f_m \rangle|^2 \to I_{nm}(t,a) \equiv \int_0^\infty \int_{-\infty}^\infty \sigma^2(T,D) \left| A_{nm}\left(a(T-t), \frac{D}{a}\right) \right|^2 \frac{dT\,dD}{D^2}. \tag{5.12}$$

Note that failure of this model (i.e., if the sources are correlated in some sense) generally will lead to image artifacts in the form of cross terms.

Equation 5.12 may be interpreted as a (perhaps more meaningful) relationship between cross-ambiguity functions and densities. There is a similarity between A_{nm} and the short-time Fourier transform. In Equation 5.6 the part of the "window function" is played by $w_m(t) = s_m(t)e^{i\omega_0 t}$, and so the density appears as a generalization of the spectrogram:

$$|A_{ss}(t,a)|^2 = a\int_{-\infty}^{\infty}\int_{-\infty}^{\infty} w_s^*(a(u+t))w_s(a(u+t+\tau))s_m(u)s_m^*(u+\tau)e^{-i\omega_o\tau}\,du\,d\tau\ . \quad (5.13)$$

Comparing this with

$$P\left(at,\frac{\omega_o}{a}\right)=\frac{1}{4\pi^2}\int_{-\infty}^{\infty}\int_{-\infty}^{\infty}\int_{-\infty}^{\infty}\phi(\theta,\tau)w^*(v)w(v+\tau)e^{i\theta(v-at)}e^{-i\tau\omega_o/a}\,dv\,d\theta\,d\tau \quad (5.14)$$

yields (after a suitable change of variables)

$$\int_{-\infty}^{\infty}\phi(\theta,\tau)e^{i\theta u}d\theta=\frac{2\pi}{a}s_m\left(\frac{u}{a}\right)s_m^*\left(\frac{u+\tau}{a}\right), \quad (5.15)$$

or

$$\phi\left(\frac{\theta}{a},a\tau\right)=\int_{-\infty}^{\infty}s_m(u)s_m^*(u+\tau)e^{-i\theta u}du\ . \quad (5.16)$$

This is the kernel for the spectrogram (properly time-scaled as in Table 4.1) and so it is instructive to compare Equation 5.15 with the kernel (Equation 4.8) obtained for the spectrogram.

As discussed in Example 4.4, one of the problems with the spectrogram is its dependence upon a predetermined size of the window function for estimating properties of the signal. If the signal varies slowly in comparison to the extent of the window, then the estimate will generally be good. However, if the signal varies rapidly within the window, then the estimate may be poor. Equation 5.15 shows that the so-called *scaleogram* of Equation 5.13 offers an interesting "solution" to this problem. Here, a fixed-shape window $s_m(t)$ will be time-scaled by the factor a^{-1} in such a way that when the signal varies rapidly (scale decreases) the window extent will be correspondingly decreased. Similarly, when the signal varies slowly, the extent of the window will be correspondingly increased. This ideal is at the heart of scale-based signal processing and has been the focus of considerable research activity (References 19 through 21).

6. CHOICE OF SIGNALS

Because of the imaging kernels (A_{mn} or $|A_{mn}|^2$), the main problem of high-resolution radar imagery is that of choosing a pulse $w_m(t)$ and a radar signal $w_n(t)$ that are most appropriate to a specific imaging application.

Recall that we are concerned with the *envelope* $s(t)$ of the waveform $w(t) = s(t)e^{i\omega_0 t}$. For actual radar systems, both the pulse and the signal will be real-valued and we can think of $s_m(t)$ and $s_n(t)$ as being the complex-valued waveforms *whose real parts* are the actual pulse envelope $h_m(t)$ and radar signal envelope $h_n(t)$, respectively. For such $h(t)$, we have $\hat{h}(-\omega) = \hat{h}^*(\omega)$ so that $h(t)$ is completely determined by its positive spectrum. It is useful to define

$$s(t) \equiv 2\int_0^\infty \hat{h}(\omega)e^{i\omega t}\,d\omega\,, \tag{6.1}$$

where the real and imaginary parts of $s(t)$ are a Hilbert transform pair and the factor of 2 guarantees that $s(t)$ and $h(t)$ have the same energy. [When the spectrum of $s(t)$ has positive support, then the *quadrature model* for $w(t)$ yields the same results (Reference 22).] Consequently, we can identify the Hardy space $H^2(R) = \{s \in L^2(R): \mathrm{supp}(\hat{s}) \subset [0,\infty)\}$ with the space of all real-valued functions in $L^2(R)$ (Reference 19). $H^2(R)$ is a closed subspace of $L^2(R)$.

The ideal imaging kernel will be one that is sharply peaked at $(\tau,a) = (0,1)$ and zero everywhere else. There are limits to how well this may be realized, however, and it is well known that matched Gaussians are the "optimal" $w_m(t)$ and $w_n(t)$ for narrowband ambiguity functions (optimal in the sense that they minimize the uncertainty relation). Unfortunately, Gaussians do not belong to $H^2(R)$. What is required for any good choice of $w(t)$ is (Reference 19):

i) $w \in H^2(R)$

ii) $w(t)$ satisfies the *admissibility condition* $\int_0^\infty \frac{|\hat{w}(\omega)|^2}{\omega}\,d\omega < \infty$. [As we shall see below, this is required if we are to recover $\rho(T,D)$ from $\langle e_n, f_m\rangle(t,a)$, or $\sigma^2(T,D)$ from $I_{mn}(t,a)$.]

Note that while a Gaussian does not belong to $H^2(R)$, the function $e^{i\omega_o t}\exp\left(-\frac{1}{2}t^2\right)$ is very close to being admissible when ω_o is sufficiently large. This suggests that matched Gaussians (or matched Gaussian-like functions) can be expected to hold an analogous role in the theory of wideband ambiguity functions. In fact, Grossman and Morlet (Reference 19) have identified the envelope that "... plays—in the H^2-theory that we are concerned with—the same privileged role that the Gaussian plays in L^2-theory." For $\beta > 0$, the function is defined by its Fourier transform as

$$\hat{s}_\beta(\omega) = \begin{cases} C_\beta \exp\left(-\frac{1}{2}\beta \ln^2 \omega\right) & \text{for } \omega > 0, \\ 0 & \text{for } \omega \le 0. \end{cases} \tag{6.2}$$

[C_β is a normalization constant: $C_\beta^2 = \sqrt{\beta/\pi}\exp(-1/4\beta)$.]

If we choose $w_m(t) = e^{ia\omega_o t} s_m(t)$ and $w_n(t) = e^{i\omega_o t} s_n(t)$, then the ambiguity function for these waveforms becomes

$$A_{nm}(\tau, a) = C_{\beta_n} C_{\beta_m} \sqrt{a}\, e^{ia\omega_o \tau} \int_0^\infty e^{ia\tau\omega} \exp\left(-\tfrac{1}{2}\beta_n \ln^2 \omega - \tfrac{1}{2}\beta_m \ln^2(a\omega)\right) d\omega. \tag{6.3}$$

Expanding the $\ln^2(a\omega)$ term in the argument shows that the waveforms will be *matched* if $\beta_n = \beta_m = \beta$. In this case, we obtain some simplification and can write

$$A_{nm}(\tau, a) = e^{ia\omega_o \tau} \sqrt{\frac{\beta}{\pi}} \exp\left(-\frac{1}{4\beta} - \frac{\beta}{4}\ln^2 a\right) \int_0^\infty e^{i\sqrt{a}\,\tau\omega} e^{-\beta \ln^2 \omega}\, d\omega \tag{6.4}$$

(which must be determined numerically.) A plot of $|A_{nm}(\tau, a)|^2$ for $\beta = 1$ is given in Figure 6.1.

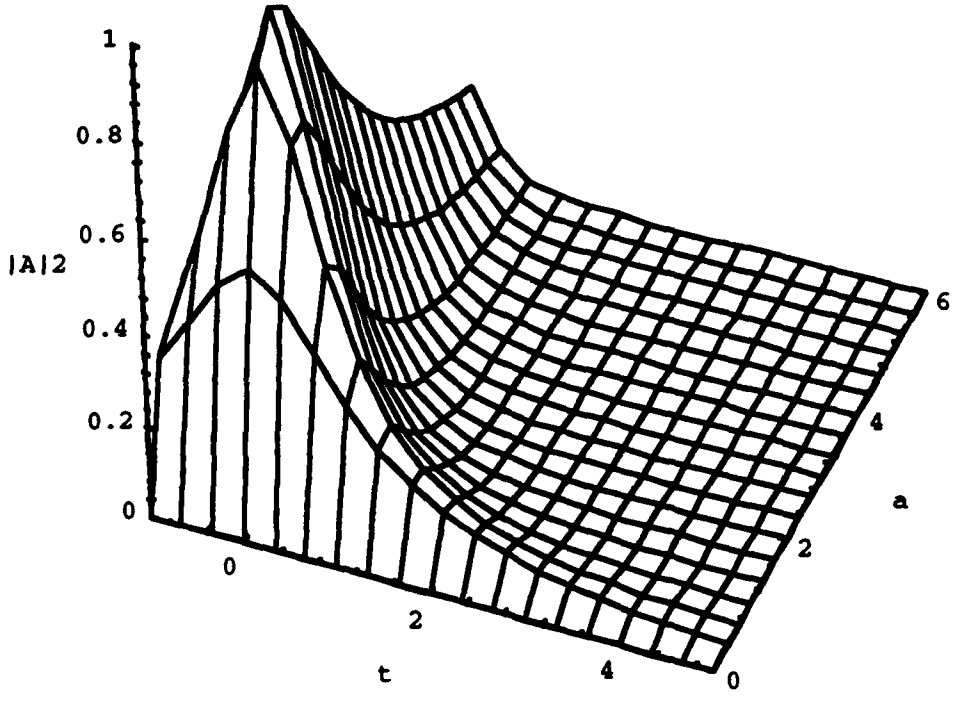

FIGURE 6.1. Wideband Ambiguity Function for $\hat{s}_\beta(\omega) = C_\beta \exp\left(-\frac{1}{2}\beta \ln^2 \omega\right)$ With $\beta = 1$.

The parameter β effectively determines the signal bandwidth. This, of course, determines the resolution to which the imaging kernel can represent the image, as can be seen by examining Figures 6.2 and 6.3. Smaller β means (practically) larger bandwidth with corresponding greater time resolution (but at the cost of scale resolution). For comparison purposes, the narrowband ambiguity function for $\hat{s}_\beta(\omega) = D_\beta \exp\left(-\frac{1}{2}\beta \omega^2\right)$ is displayed in Figures 6.4 through 6.6.

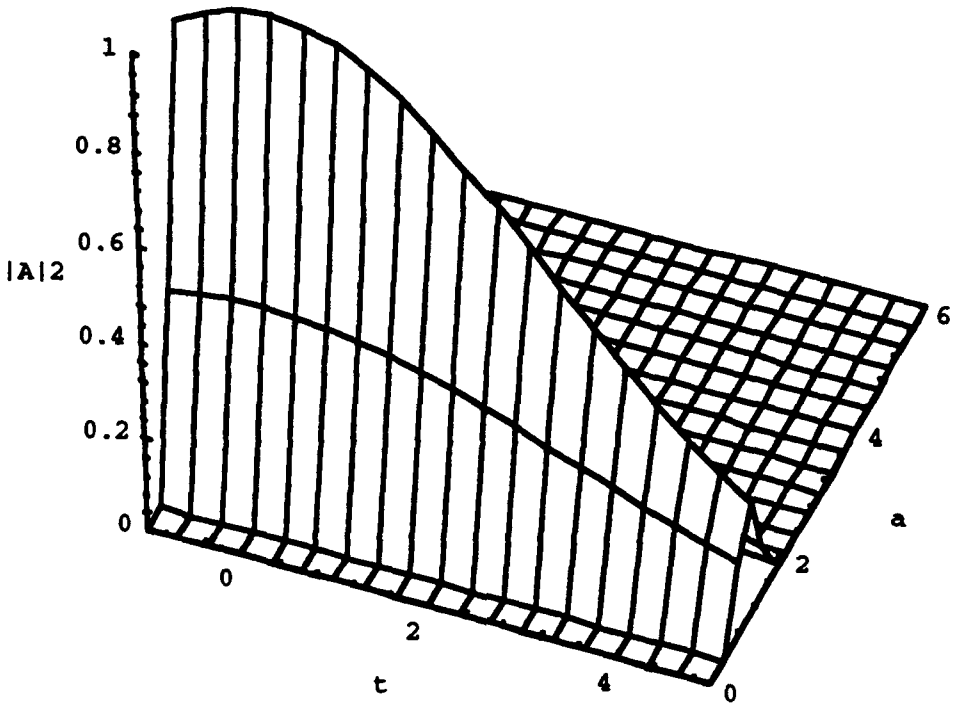

FIGURE 6.2. Wideband Ambiguity Function for $\hat{s}_\beta(\omega) = C_\beta \exp\left(-\frac{1}{2}\beta \ln^2 \omega\right)$ With $\beta = 10$.

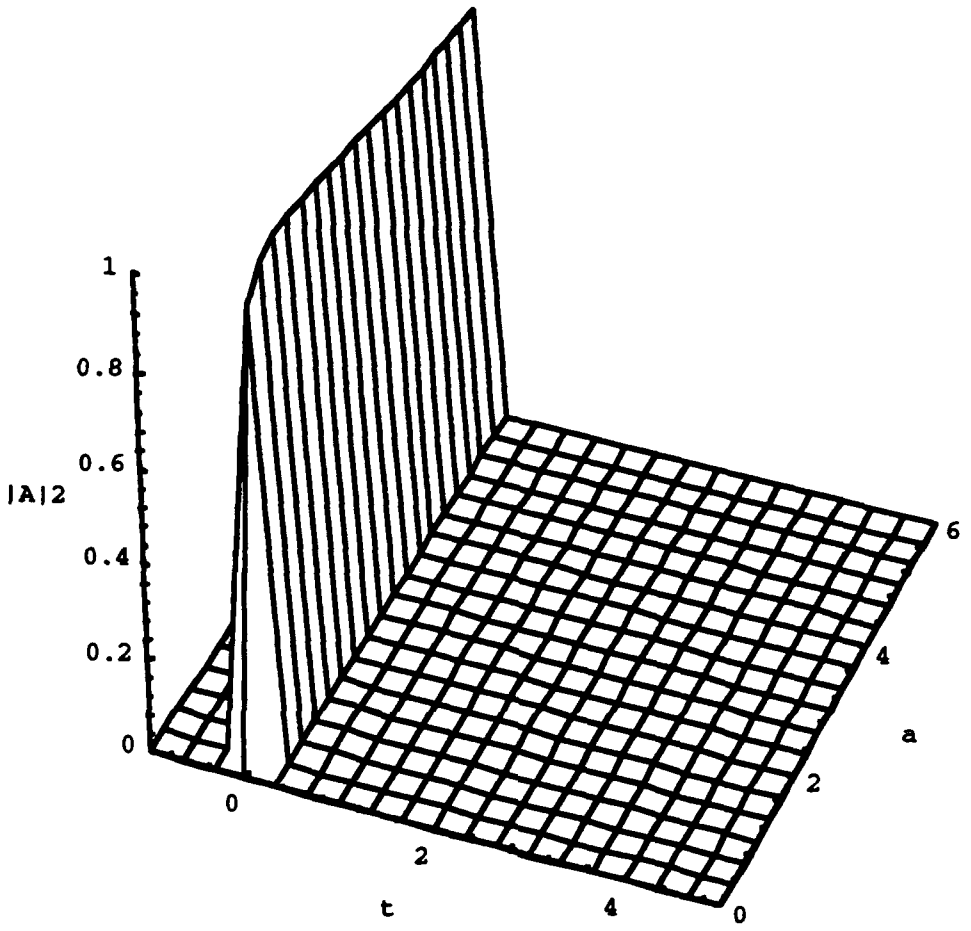

FIGURE 6.3. Wideband Ambiguity Function for $\hat{s}_\beta(\omega) = C_\beta \exp\left(-\frac{1}{2}\beta \ln^2 \omega\right)$ With $\beta = 1/10$.

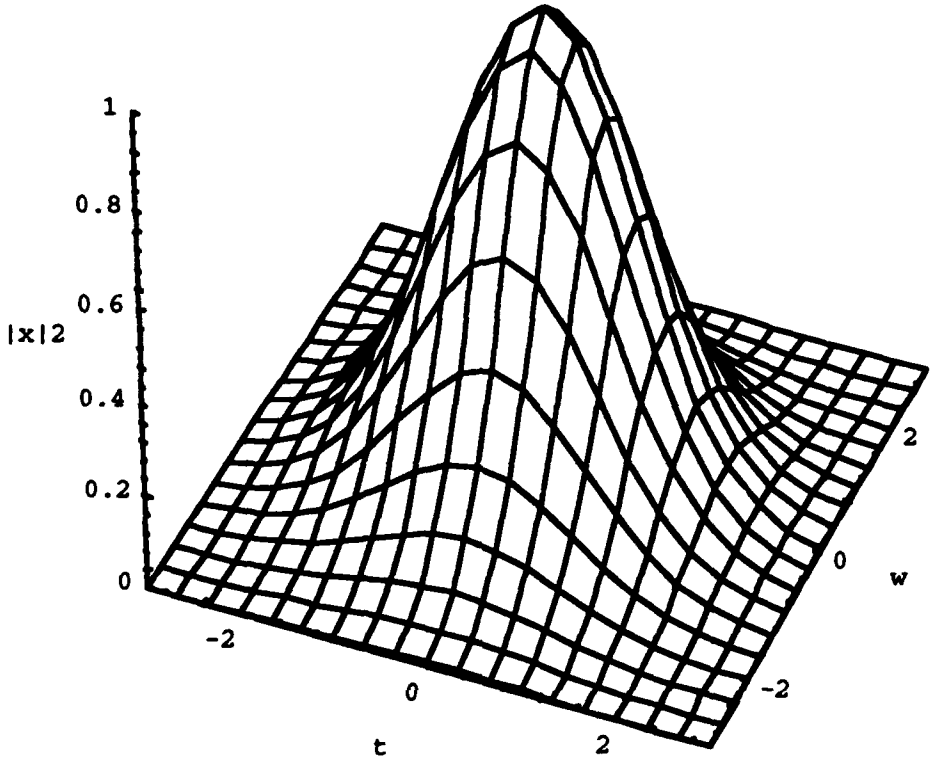

FIGURE 6.4. Narrowband Ambiguity Function $|\chi_{mn}|^2$ for $\hat{s}_\beta(\omega) = D_\beta \exp\left(-\frac{1}{2}\beta\omega^2\right)$ With $\beta = 1$.

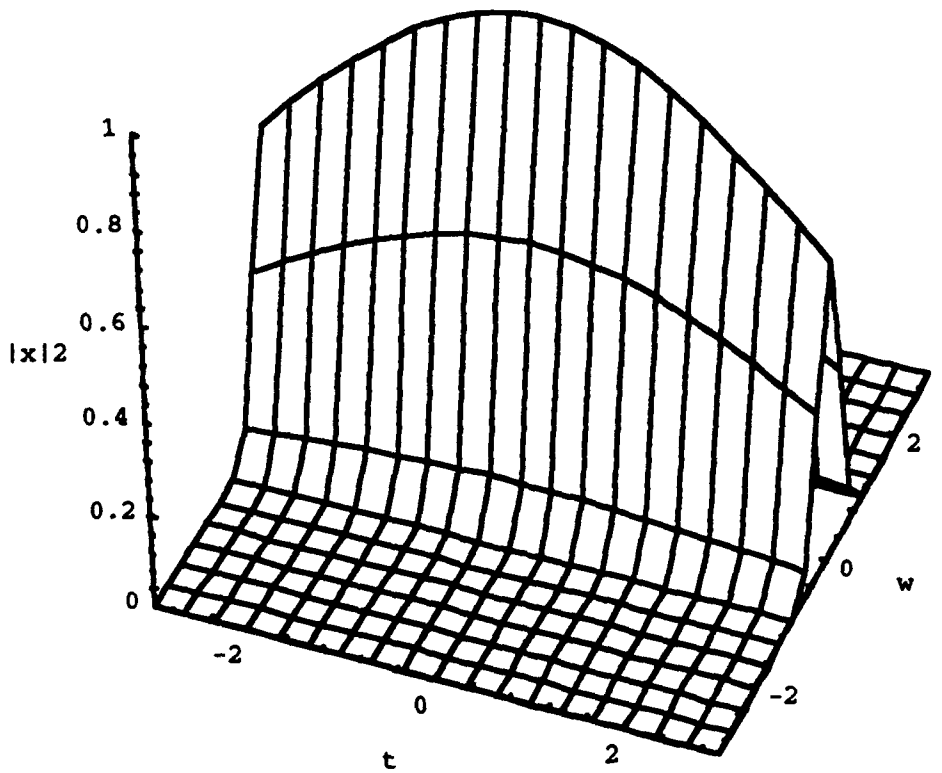

FIGURE 6.5. Narrowband Ambiguity Function for $\hat{s}_\beta(\omega) = D_\beta \exp\left(-\frac{1}{2}\beta\omega^2\right)$ With $\beta = 10$.

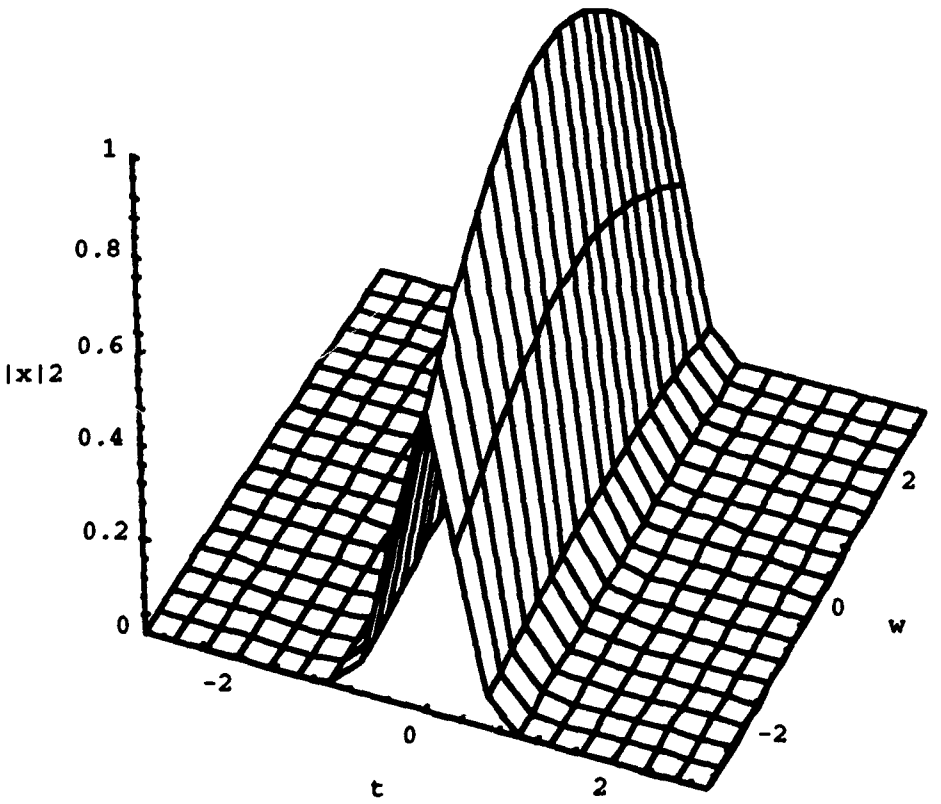

FIGURE 6.6. Narrowband Ambiguity Function for $\hat{s}_\beta(\omega) = D_\beta \exp\left(-\frac{1}{2}\beta\omega^2\right)$ With $\beta = 1/10$.

Of course, to be accurate, we really want neither the reflectivity image $\langle e_n, f_m \rangle(t,a)$ nor the intensity image $I_{mn}(t,a)$; rather, we desire the reflectivity density $\rho(T,D)$ or the cross-section density $\sigma^2(T,D)$. These densities are directly related to the target properties alone, and to get at them we must choose signals that lead to imaging kernels that are invertible.

The reflectivity image is given by

$$\langle e_n, f_m \rangle(t,a) = \int_0^\infty \int_{-\infty}^{\infty} \rho(T,D) A_{mn}\left(a(T-t), \frac{D}{a}\right) \frac{dT\, dD}{D} . \tag{6.5}$$

Clearly, we need to find some $B_{jk}(\tau,\alpha)$ such that

$$\rho(T',D') = \int_0^{\infty}\int_{-\infty}^{\infty} \langle e_n, f_m \rangle (t,a) B_{jk}^{*}\left(a(T'-t), \frac{D'}{a}\right)\frac{dt\,da}{a} . \tag{6.6}$$

If we write $B_{jk}(\tau,\alpha)$ in the form

$$B_{jk}(\tau,\alpha) = \sqrt{\alpha}\int_{-\infty}^{\infty} w_j(\alpha(u+\tau))w_k^{*}(u)du , \tag{6.7}$$

then it is straightforward to show that our inversion requirement becomes

$$\rho(T',D') = \int_0^{\infty}\frac{\hat{w}_k(\omega)\hat{w}_m^{*}(\omega)}{\omega}d\omega \int_0^{\infty}\int_{-\infty}^{\infty}\rho(T,D)A_{nj}\left(D'(T-T'), \frac{D}{D'}\right)\frac{dT\,dD}{D} . \tag{6.8}$$

If $w_k = w_m$, then the admissibility condition shows that this is a well-defined operation. However, we are back to the original problem of seeking an ideal ambiguity function $A_{nj}(\tau,a)$ that is sharply peaked at $(\tau,a) = (0,1)$ and zero everywhere else.

7. WHY GO WIDEBAND?

While the constraint on the duration-bandwidth product (the uncertainty principle) guarantees that we can never achieve the optimal imaging kernel $A_{nj}(\tau,a) = \delta(\tau)\delta(a-1)$, we *are* able to obtain $A_{nj}(\tau,a) = \delta(\tau)$ or $A_{nj}(\tau,a) = \delta(a-1)$. In fact, since we can make multiple radar measurements of the same system, we could follow a measurement using the waveform described in Figure 6.2 (Figure 6.5) with a second measurement using the waveform of Figure 6.3 (Figure 6.6). Correlating such ideal measurements allows us to achieve as much imaging resolution as we might desire. In either of these measurements we are free to choose from a wide variety of waveforms $w(t)$, since we no longer seek to "optimize" against some uncertainty constraint. This freedom in choice of $w(t)$ means

that we can select a waveform that is suited to other aspects of the particular problem at hand.

Even when we are not planning such correlated measurement imaging, we still are particularly interested in high-resolution downrange imaging, since this information might be used more readily for target imaging than cross-range (Doppler) information. In either case, however, we are interested in those $w(t)$ that have very narrow envelopes $s(t)$, since these so-called *wideband* waveforms allow for very fine downrange resolution of radar targets. (In contrast, narrowband signals provide low downrange resolution.) Much of the intuition developed from experience with ordinary (narrowband) radar systems carries over directly to the wideband case. In general, however, the narrowband ambiguity function may not be a completely accurate imaging kernel for rapidly moving targets. Note also that the narrowband ambiguity function is related to the Wigner distribution, while the wideband ambiguity function does not enjoy the same relationship. However, we can dismiss any vague concern that Fourier methods may not apply to wideband radars. As we have seen, Fourier methods work just fine in the present analysis—provided that they are applied correctly.

To understand better the differences between the two approaches and to quantify the possible loss in (narrowband) imaging accuracy, we shall compare $A_{mn}(\tau,a)$ with $\chi_{mn}(t,\omega)$ for various bandwidths. If we set $w_n(t)=w_m(t)=e^{i\omega_o t}s(t)$ then, in terms of the narrowband imaging kernel, we can write

$$\begin{aligned}\tilde{\chi}(t,(a-1)\omega_o) &\equiv 2\pi\sqrt{a}\,e^{i\omega_o t}\chi_{nn}(t,(a-1)\omega_o)\\ &= \sqrt{a}\,e^{i\omega_o t}\int_{-\infty}^{\infty} s(u+t)s^*(u)e^{i(a-1)\omega_o u}\,du\\ &= \sqrt{a}\,e^{i\omega_o t}\int_{-\infty}^{\infty} \hat{s}(\omega)\hat{s}^*(\omega-(1-a)\omega_o)e^{i\omega t}\,d\omega.\end{aligned} \tag{7.1}$$

Whereas, the corresponding wideband imaging kernel is

$$\begin{aligned}A(t/a,a) \equiv A_{mn}(t/a,a) &= \sqrt{a}\,e^{i\omega_o t}\int_{-\infty}^{\infty} s(au+t)s^*(u)e^{i(a-1)\omega_o u}\,du\\ &= \sqrt{a}\,e^{i\omega_o t}\int_{-\infty}^{\infty} \hat{s}(\omega)\hat{s}^*(a\omega-(1-a)\omega_o)e^{i\omega t}\,d\omega.\end{aligned} \tag{7.2}$$

As a concrete example, consider the Gaussian waveform $\hat{s}(\omega) = D_\beta \exp\left(-\tfrac{1}{2}\beta\omega^2\right)$. This waveform is computationally easy to deal with and is almost in $H^2(R)$ when ω_o is sufficiently large—say $\omega_o \geq$ Bandwidth / 2. [In this case, it is appropriate to use the *Woodward Bandwidth* (Reference 23):

$$B_W^2 = \int_{-\infty}^{\infty} \omega^2 |\hat{s}(\omega)|^2 \, d\omega = D_\beta^2 \int_{-\infty}^{\infty} \omega^2 e^{-\beta\omega^2} \, d\omega = \frac{1}{2\beta} , \tag{7.3}$$

since $D_\beta^2 = \sqrt{\beta / \pi}$.] Substitution of this Gaussian waveform into Equations 7.1 and 7.2 yields

$$\begin{aligned} \tilde{\chi}(t,(a-1)\omega_o) &= \sqrt{\frac{\beta a}{\pi}} e^{i\omega_o t} \exp\left(-\tfrac{1}{2}\beta(1-a)^2\omega_o^2\right) \int_{-\infty}^{\infty} \exp\left[-\beta\omega^2 + (\beta\omega_o(1-a)+it)\omega\right] d\omega \\ &= \sqrt{a} \exp\left(i\frac{3-a}{2}\omega_o t\right) \exp\left(-\tfrac{1}{2}\beta(1-a)^2\omega_o^2\right) \exp\left(-\frac{t^2-(1-a)^2\beta^2\omega_o^2}{4\beta}\right) \end{aligned} \tag{7.4}$$

and

$$\begin{aligned} A\left(\frac{t}{a},a\right) &= \sqrt{\frac{\beta a}{\pi}} e^{i\omega_o t} \exp\left(-\tfrac{1}{2}\beta(1-a)^2\omega_o^2\right) \int_{-\infty}^{\infty} \exp\left[-\tfrac{1}{2}\beta\left(1+a^2\right)\omega^2 + (\beta\omega_o a(1+a)+it)\omega\right] d\omega \\ &= \sqrt{\frac{2a}{1+a^2}} \exp\left(i\frac{1+a}{1+a^2}\omega_o t\right) \exp\left(-\tfrac{1}{2}\beta(1-a)^2\omega_o^2\right) \exp\left(-\frac{t^2-a^2(1-a)^2\beta^2\omega_o^2}{2\beta\left(1+a^2\right)}\right). \end{aligned} \tag{7.5}$$

For fixed a, the scatterer location (in time) will be estimated by the maximum of the respective ambiguity functions. If t_A denotes the estimate from the wideband ambiguity function $A(t/a,a)$ and t_χ the narrowband ambiguity function $\tilde{\chi}(t,(1-a)\omega_o)$ estimate, then it is easy to see that

$$t_A - t_\chi = -(1-a)^2 \beta \omega_o = -\frac{(1-a)^2}{4B_W} \tag{7.6}$$

for $\omega_o = \frac{1}{2}B_W$. This difference vanishes when the target is not moving ($a = 1$). However, downrange distances of moving targets will be overestimated by the narrowband ambiguity function. But this error is usually not significant: if the target velocity obeys $|v| << c$; hence,

$$t_A - t_\chi \approx -\frac{v^2}{4B_W c^2} . \tag{7.7}$$

(We can show that the phase error is similarly insignificant, but the phase term is usually ignored.)

In the narrowband case, it is still true that increasing bandwidth will increase time resolution. The example shows that when $\hat{s}(\omega)$ is chosen to be symmetric and centered on $\omega_o \geq \frac{1}{2}B_W$ there is little difference between the wideband and narrowband results (at least as far as radar systems are concerned). This is, perhaps, why the "widebandness" of radar is sometimes defined by the ratio of bandwidth to center frequency.

In the Hardy space case, no such minimum size restrictions for ω_o exist; however, it is important to remember that these waveforms should be elements of Hardy space. This requirement guarantees that we will not have any unexpected artifacts obtained by trying to represent functions that are members of $H^2(R)$ by elements of $L^2(R)$. Moreover, often it may be advantageous to consider proper waveforms (i.e., with nonsymmetric spectra) for radar-detection applications (c.f., Reference 21). In this case, the differences between the narrowband and wideband imaging kernels may become significant because of the way the imaging kernel is sharpened when $\alpha < 1$.

8. CONCLUSION

It is not surprising that, for radar applications, the wideband and narrowband ambiguity functions should yield such close results. After all, they only differ by terms of order v/c. Moreover, if there were serious errors in the way the narrowband ambiguity functions performed, then surely they would have been discovered in a half-century of radar-system development. (Sonar applications are another matter, however,

and all of these results carry over to acoustic sensing but with the possibility that v/c can, in practice, become significantly large.)

However, we should not conclude that wideband ambiguity functions are merely a mathematical curiosity. The narrowband analysis does not tell the entire story, and intuition gained from it is not complete. The shift in attention from time-frequency to time-scale representations is made natural by the shift from narrowband to wideband ambiguity functions. In turn, the representation of signals by affine covariant states (wavelets) holds the potential for significantly improving the imaging capabilities of future radar (and sonar) systems (c.f., Reference 21 and references cited therein).

Current work has been concentrated on demonstrating the utility of this approach using actual and simulated frequency domain data. Stepped frequency data collected over large bandwidths have been in use for many years, and filtering techniques allow for easy modification to the present purposes.

Current plans for future work include a detailed investigation into appropriate choices for radar waveforms, as well as practical techniques for generating them in the time-domain.

Appendix

MOTIVATION FOR THE MEASURE $dT\,dD\,/\,D$

In the narrowband case, the equivalent to Equation 5.9 can be written

$$\langle e,f\rangle(t,\omega) = \int_{-\infty}^{\infty}\int_{-\infty}^{\infty}\rho(T,\Omega)\chi(T-t,\Omega-\omega)dT\,d\Omega\ . \tag{A.1}$$

This is a correlation integral between ρ and χ, and so obeys the (Fourier) correlation theorem:

$$\int_{-\infty}^{\infty} g(x')h(x'+x)dx' \underset{F}{\Leftrightarrow} \hat{g}(y)\hat{h}^{*}(y)\,, \tag{A.2}$$

where $\underset{F}{\Leftrightarrow}$ denotes Fourier transformation. We would like Equation 5.9 to also obey a correlation property. The measure choice $dx\,/\,x$ allows us to do this, since under the Mellin transform (Reference 24),

$$\int_{0}^{\infty} g(x')h\left(\frac{x'}{x}\right)\frac{dx'}{x'} \underset{M}{\Leftrightarrow} \tilde{g}(y)\tilde{h}(-y)\ , \tag{A.3}$$

where $\underset{M}{\Leftrightarrow}$ denotes the Mellin transformation:

$$\tilde{g}(y) \equiv \int_0^\infty g(x) x^{y-1} dx \ . \tag{A.4}$$

Alternately, we can avoid any mention of Mellin transforms and force integrals of the type in Equation A.3 to appear to be the kind of correlation integrals we are used to. This can be accomplished by making the change of variables $x \rightarrow e^u$, which yields

$$\int_0^\infty g(x') h\left(\frac{x'}{x}\right) \frac{dx'}{x'} \ \rightarrow \ \int_{-\infty}^\infty G(u') H(u'-u) du' \ , \tag{A.5}$$

where $G(u) \equiv g(e^u)$. (This approach is used in Reference 19.)

Independent of the motivation for this choice of measure, the consequences have been important for us. It was this measure that was responsible for the signal admissibility condition of Section 6 and for the logarithm appearing in the argument of Equation 6.2.

REFERENCES

1. H. Naparst. "Dense Target Signal Processing," *IEEE Trans. Inf. Theory*, Vol. 37 (1991), pp. 317-27.

2. E. G. Kalnins and W. Miller, Jr. "A Note on Group Contractions and Radar Ambiguity Functions," in *Institute for Math. and Its Applications, Radar and Sonar*. New York, Springer-Verlag, 1992. Vol. 39, pp. 71-82.

3. P. Maass. "Wideband Approximation and Wavelet Transform," *ibid.*, pp. 83-88.

4. L. Cohen. "Time-Frequency Distributions—A Review," *Proc. IEEE*, Vol. 77 (1989), pp. 941-81.

5. -------. "Generalized Phase-Space Distribution Functions," *J. Math. Phys.*, Vol. 7 (1966), pp. 781-86.

6. E. P. Wigner. "On the Quantum Correction for Thermodynamic Equilibrium," *Phys. Rev.*, Vol. 40 (1932), pp. 749-59.

7. J. Ville. "Théorie et Applications de la Notion de Signal Analytique," *Cables et Transmission*, Vol. 2A (1948), pp. 61-74.

8. T.A.C.M. Claasen and W.F.G. Mecklenbräuker. "The Wigner Distribution—A Tool for Time-Frequency Signal Analysis, " *Phillips J. Res.*, Vol. 35 (1980), pp. 372-89.

9. H. I. Choi and W. J. Williams. "Improved Time-Frequency Representations of Multicomponent Signals Using Exponential Kernels," *IEEE Trans. Acoust., Speech, Signal Proc.*, Vol. 37 (1989), pp. 862-71.

10. J. G. Kirkwood. "Quantum Statistics of Almost Classical Ensembles," *Phys. Rev.*, Vol. 44 (1933), pp. 31-37.

11. W. Rihaczek. "Signal Energy Distribution in Time and Frequency," *IEEE Trans. Inf. Theory*, Vol. 14 (1968), pp. 369-74.

12. L. Cohen and T. Posch. "Positive Time-Frequency Distribution Functions," *IEEE Trans. Acoust., Speech, Signal Proc.*, Vol. 33 (1985), pp. 31-38.

13. P. D. Finch and R. Groblicki. "Bivariate Probability Densities With Given Marginals," *Found. Phys.*, Vol. 14 (1984), pp. 549-52.

14. L. Mandel. "Interpretation of Instantaneous Frequency," *Am. J. Phys.*, Vol. 42 (1974), pp. 840-46.

15. E. J. Kelly and R. P. Wishner. "Matched-Filter Theory for High-Velocity, Accelerating Targets," *IEEE Trans. Military Elec.*, Vol. 9 (1965), pp. 56-69.

16. C. E. Cook and M. Bernfeld. *Radar Signals*. New York, Academic Press, 1967.

17. Naval Research Laboratory. *A Review of Wideband Ambiguity Functions*, by D. A. Swick. Arlington, VA, NRL, 1969. (NRL Report 6994.)

18. L. Cohen and T. E. Posch. "Generalized Ambiguity Functions," in *International Conference on Acoust., Speech, Signal Proc.*, Vol. 85 (1985), pp. 1033-36.

19. A. Grossmann and J. Morlet. "Decomposition of Hardy Functions Into Square Integrable Wavelets of Constant Shape," *SIAM J. Math. Anal.*, Vol. 15 (1984), pp. 723-36.

20. P. Flandrin and O. Rioul. "Affine Smoothing of the Wigner-Ville Distribution," in *International Conference on Acoust., Speech, Signal Proc.*, Vol. 90 (1990), pp. 2455-58.

21. I. Daubechies. "The Wavelet Transform, Time-Frequency Localization, and Signal Analysis," *IEEE Trans. Inf. Theory*, Vol. 36 (1990), pp. 961-1005.

22. A. H. Nuttall. "On the Quadrature Approximation to the Hilbert Transform of Modulated Signals," *Proc. IEEE*, Vol. 54 (1966), pp. 1458-59.

23. P. M. Woodward. *Probability and Information Theory With Applications to Radar*. London, Pergamon, 1964.

24. A. Erdelyi and others. *Tables of Integral Transforms*. New York, McGraw-Hill, 1955.

INITIAL DISTRIBUTION

2 Naval Air Systems Command
  AIR-933B (1)
  AIR-933E, D. Glista (1)
4 Chief of Naval Research
  J. Cauffman (1)
  Dr. K. Davis (1)
  Dr. R. Madan (1)
  W. Miceli (1)
1 Naval Sea Systems Command (C. E. Jedrey)
1 Commander in Chief, U. S. Pacific Fleet, Pearl Harobr (Code 325)
1 Commander, Third Fleet
1 Commander, Seventh Fleet
2 Naval Air Warfare Center, Aircraft Division, Warminster
  Code 3022, Dr. O. Kessler (1)
  Technical Library (1)
4 Naval Command Control and Ocean Surveillance Center, RDTE Division, San Diego
  R. J. Dingar (1)
  P. Hansen (1)
  C. Ramstadt (1)
  Technical Library (1)
2 Naval Postgraduate School, Monterey, CA
  Dr. M. A. Morgan (1)
  Technical Library (1)
5 Naval Research Laboratory
  Code 7500, Dr. J. R. Davis (1)
  Code 7550
    D. Himes (1)
    L. Wagner (1)
  Dr. A. Jordan (1)
  Technical Library (1)
1 Naval War College, Newport
1 Air Force Intelligence Support Agency/Directorate of Targets, Bolling Air Force Base (AFISA/INT)
2 Defense Technical Information Center, Alexandria
1 A. J. Devaney Associates, Ridgefield, CT (Dr. A. J. Devaney)
1 General Dynamics Corporation, San Diego, CA (Dr. C. P. Tricoles)
1 Center for Naval Analyses, Alexandria, VA (Technical Library)
1 Institute for Defense Analyses, Alexandria, VA (Dr. I. Kay)
2 Massachusetts Institute of Technology, Lincoln Laboratory, Lexington, MA
  Dr. R. M. Barnes (1)
  Dr. G. Morse (1)
1 Michigan State University, East Lansing, MI (Prof. K. M. Chen)
1 Ohio State University, Columbus, OH (Dr. E. Walton)
1 University of Illinois, Chicago, IL (Dr. W. Boerner)